Overexpression of EZH2 in conjunctival melanoma offers a new therapeutic target

Cao, J.; Pontes, K.C.S.; Heijkants, R.C.; Brouwer, N.J.; Groenewoud, A.; Jordanova, E.S.; ... ; Jager, M.J.

Journal of Pathology
J Pathol 2018; **245:** 433–444
Published online 23 June 2018 in Wiley Online Library (wileyonlinelibrary.com) DOI: 10.1002/path.5094

ORIGINAL PAPER

Overexpression of EZH2 in conjunctival melanoma offers a new therapeutic target

Jinfeng Cao[1,2], Kelly CS Pontes[1,3], Renier C Heijkants[4], Niels J Brouwer[1], Arwin Groenewoud[3], Ekaterina S Jordanova[5,6], Marina Marinkovic[1], Sjoerd van Duinen[5], Amina FAS Teunisse[4], Robert M Verdijk[7], Ewa Snaar-Jagalska[3], Aart G Jochemsen[4†] and Martine J Jager[1*†]

[1] *Department of Ophthalmology, Leiden University Medical Centre, Leiden, The Netherlands*
[2] *Department of Ophthalmology, The Second Hospital of Jilin University, Changchun, PR China*
[3] *Department of Molecular Cell Biology, Institute of Biology, Leiden University, Leiden, The Netherlands*
[4] *Department of Molecular Cell Biology, Leiden University Medical Centre, Leiden, The Netherlands*
[5] *Department of Pathology, Leiden University Medical Centre, Leiden, The Netherlands*
[6] *Centre for Gynaecological Oncology Amsterdam (CGOA), VU University Medical Centre, Amsterdam, The Netherlands*
[7] *Department of Pathology, Section Ophthalmic Pathology, Erasmus MC University Medical Centre, Rotterdam, The Netherlands*

**Correspondence to: Professor Dr Martine J Jager, Department of Ophthalmology, Leiden University Medical Centre, PO Box 9600, 2300 RC Leiden, The Netherlands. E-mail: m.j.jager@lumc.nl*

†MJJ and AGJ are co-senior authors.

Abstract

Malignant melanoma of the conjunctiva (CM) is an uncommon but potentially deadly disorder. Many malignancies show an increased activity of the epigenetic modifier enhancer of zeste homolog 2 (EZH2). We studied whether EZH2 is expressed in CM, and whether it may be a target for therapy in this malignancy. Immunohistochemical analysis showed that EZH2 protein expression was absent in normal conjunctival melanocytes and primary acquired melanosis, while EZH2 was highly expressed in 13 (50%) of 26 primary CM and seven (88%) of eight lymph node metastases. Increased expression was positively associated with tumour thickness ($p=0.03$). Next, we targeted EZH2 with specific inhibitors (GSK503 and UNC1999) or depleted *EZH2* by stable shRNA knockdown in three primary CM cell lines. Both pharmacological and genetic inactivation of EZH2 inhibited cell growth and colony formation and influenced EZH2-mediated gene transcription and cell cycle profile *in vitro*. The tumour suppressor gene *p21/CDKN1A* was especially upregulated in CM cells after *EZH2* knockdown in CM cells. Additionally, the potency of GSK503 against CM cells was monitored in zebrafish xenografts. GSK503 profoundly attenuated tumour growth in CM xenografts at a well-tolerated concentration. Our results indicate that elevated levels of EZH2 are relevant to CM tumourigenesis and progression, and that EZH2 may become a potential therapeutic target for patients with CM.

Keywords: conjunctival melanoma; primary acquired melanosis; EZH2; histone methylation; cell death; zebrafish

Received 19 November 2017; Revised 23 March 2018; Accepted 27 April 2018

No conflicts of interest were declared.

Introduction

Conjunctival melanoma (CM) is a rare malignancy on the ocular surface, showing an increasing incidence in Europe and the United States [1–3]. CMs recur frequently after surgical removal and can lead to death, due to metastases [4,5]. The melanoma-related death rate can reach 29% at 10 years [5,6]. Once distant metastases occur, there are few therapeutic options.

CMs share many characteristics with cutaneous melanoma, such as the presence of *BRAF* or *NRAS* mutations, which occur in 29% and 18% of CMs, respectively, and lead to activation of the MAPK pathway [7]. We recently showed that BRAF inhibitors are effective on *BRAF*-mutated CM cell lines [8], and at least two patients have been treated with these drugs [9,10]. As resistance to these drugs may develop, there is a need for alternative targets. In recent years, awareness has increased that not only genetic alterations but also aberrant epigenetic regulation may be the basis of malignant disorders. Many epigenetic processes are regulated through the polycomb repressive complex 2 (PRC2), and overexpression of one of its core catalytic subunits, enhancer of zeste homolog 2 (EZH2), has been observed in a broad spectrum of cancer types including cutaneous melanoma, breast cancer, and endometrial carcinoma [11,12]. EZH2 is a histone methyltransferase which catalyses trimethylation of lysine 27 in histone

H3 (H3K27me3); this leads to transcriptional silencing of many genes, including tumour suppressor genes, rendering *EZH2* a potential oncogene [13,14]. EZH2 is not expressed in the normal tissues of adults, except in actively dividing cells, such as stem cells [15]. Somatic mutations including gain-of-function alterations of *EZH2* have primarily been discovered in haematopoietic malignancies. Currently, drugs that target EZH2 have shown promising preclinical results, and some phase 1/2 clinical trials using small molecule inhibitors have been initiated for *EZH2* mutant or wild-type lymphoma [16–18].

Insight into the importance of EZH2 in melanoma is increasing [19]. Although somatic activating *EZH2* mutations occurred in only 3% of cutaneous melanomas [19], EZH2 is frequently overexpressed in cutaneous melanoma cells, while its expression is not detectable in benign naevi, suggesting a role for EZH2 in melanoma progression [20]. Furthermore, EZH2 depletion or inhibition has been shown to repress tumour growth and metastasis in a murine model of cutaneous melanoma [21]. Although in many ways CM resembles cutaneous melanoma, the study of EZH2 expression and function in a biological context of CM development is still missing.

Here, we show that EZH2 expression is absent in normal conjunctival melanocytes and primary acquired melanosis (PAM) but elevated in primary tumours and metastases of CM patients. In addition, we reveal that pharmacological inhibition of EZH2 activity or genetic depletion of *EZH2* leads to robust anti-cancer effects *in vitro* and *in vivo*. These results indicate that targeting EZH2 may provide a novel therapeutic strategy against CM.

Materials and methods

Study population

Paraffin-embedded tissue specimens of nine PAMs, 26 primary CMs, and one lymph node metastasis were collected through the archives of the Department of Pathology, Leiden University Medical Centre, Leiden, from patients who had been diagnosed with a conjunctival melanocytic lesion between 1990 and 2014. Paraffin-embedded material of seven lymph node metastases of CM was retrieved from the Department of Pathology of the Erasmus University Medical Centre. All specimens contained enough material for the study. Five normal conjunctival samples were obtained from uveal melanoma-containing enucleated eyes. The use of human materials was approved by the Ethical Committee Board of Leiden University Medical Centre and allowed by Erasmus University Medical Centre because it was a retrospective and non-interventional study. The diagnosis was reviewed, and the original slides were assessed according to the seventh edition of the *AJCC TNM Cancer Staging Manual* [21].

Immunohistochemistry (IHC) staining and evaluation

IHC was carried out as previously described [22]. In brief, after hot (100 °C) antigen retrieval in a microwave oven and 1 h cooling to room temperature, sections were blocked with normal goat serum (1:10, X0907; Dako, Glostrup, Denmark) for 1 h at room temperature, after which the slides were incubated with anti-EZH2 monoclonal antibody (1:100, 612667; BD Biosciences, Vianen, The Netherlands) overnight at 4 °C. Thereafter, slides were incubated with peroxidase-labelled polymer conjugated to a goat anti-mouse secondary antibody (K4000; Dako), visualized with a NovaRED substrate kit (SK-4800; Vector Laboratories, Burlingame, CA, USA), counterstained with haematoxylin, and mounted with Kaiser's glycerol gelatine. Human placental tissue served as the positive control. An isotype control was obtained by replacing the primary antibody with the mouse IgG1 reagent (X9031; Dako). Evaluation was done by two independent observers (JC and EJ) in a blinded manner. In cases of divergent scores, a consensus was reached by simultaneous evaluation. Images were taken using Philips Image Management System 2.2. A staining index (SI) system evaluating both intensity (0 = no staining; 1 = weak; 2 = moderate; and 3 = strong) and percentage of cells with nuclear EZH2 staining (1 = ≤ 10%; 2 = 11–50%; and 3 ≥ 50%) was used [12,23]. Multiplying intensity and percentage produced total scores (0–9). After considering the distribution plots and number of cases, the median (SI = 3) was set as the cut-off value between low expression and high expression, as previously described [12,23].

Cell lines, lentiviral transduction, and chemical reagents

Human CM cell lines CRMM1 and CRMM2 were established by G Nareyeck, Essen, Germany [24], and kindly provided by M Madigan, Sydney, Australia. CM2005.1 was established by S Keijser, LUMC, Leiden, The Netherlands [25]. Human cutaneous melanoma cell lines A375 and MEL93.05 were kindly provided by E Verdegaal, LUMC, Leiden, The Netherlands. The media and methods of cell culture have been described previously [8]. Two validated MISSION®shRNA constructs (TRCN0000040-075 and TRCN0000040-077; Sigma Aldrich, St Louis, MO, USA) were used to silence EZH2. Control shRNA vectors were from the same library, the non-targeting shc002, and the luciferase targeting shc007. HEK293T cells were transfected with the shRNA constructs together with helper plasmids encoding HIV-1 gag-pol, HIV-1 rev, and the VSV-G envelope, as described previously [26]. To determine virus titres, p24 antigen levels were determined using an HIV-1 p24 antigen enzyme-linked immunosorbent assay (ELISA) kit (ZeptoMetrix Corp, Buffalo, NY, USA). The CM cell lines were transduced with an MOI (multiplicity of infection) of 2.0 for 16 h in medium containing 8.0 μg/ml polybrene. Virus-containing medium

was replaced with fresh medium containing puromycin (1 μg/ml) for 72 h to select transduced cells. GSK503 (S7804) and UNC1999 (S7165) were purchased from Selleck Chemicals (Huissen, The Netherlands). All drugs were dissolved in dimethyl sulphoxide (DMSO) to obtain a stock solution of 20 mM.

Immunoblotting

Protein lysates were extracted using 1.5× SDS sample buffer (75 mM Tris–HCl, pH 6.8; 3% SDS; 15% glycerol). SDS-PAGE was carried out by loading 15–20 μg of total protein lysate on Mini-PROTEAN TGX Precast Gels (4–15%; Bio-Rad, Veenendaal, The Netherlands). Proteins were blotted onto polyvinylidene difluoride membranes (Immobilon-P; Millipore, Burlington, MA, USA). Next, membranes were incubated overnight with primary antibodies (supplementary material, Table S1) diluted with Odyssey blocking buffer (927-5000; LI-COR; Westburg BV, Leusden, The Netherlands) at 4 °C, and visualized using IRdye-680 or IRdye-800 secondary antibodies (LI-COR). Blots were scanned and analysed with the Odyssey Infrared Imaging System (LI-COR). Alternatively, membranes were incubated with horseradish peroxidase (HRP)-conjugated secondary antibodies and visualized by chemiluminescence.

Cell proliferation and colony assay

The in-cell western assay was used to determine the growth rate, as previously described [8]. Detailed information is given in the supplementary material, Supplementary materials and methods.

Flow cytometry, RNA isolation, cDNA synthesis, and quantitative PCR

Details are provided in the supplementary material, Supplementary materials and methods, and primer sequences are shown in the supplementary material, Table S2.

Fluorescent cell labelling and zebrafish model

To generate CM cells with red fluorescence, cells were stably transduced with lentivirus expressing both tdTomato and blasticidin-S, as described previously [27]. Virus-containing medium was replaced with fresh medium containing blasticidin-S (2 μg/ml) to select transduced cells. Transduction of the cells with the tdTomato-expressing virus did not alter the growth pattern of parental cells [28].

The (fli:GFP) Casper zebrafish embryos were maintained according to standard protocols (http://ZFIN.org, in the public domain) [29,30], in compliance with Dutch animal welfare regulations. The research followed the statement on the use of animals in research as published by the Association for Research in Vision and Ophthalmology and has been described previously [28]. To test drug toxicity, non-injected 3 days post-fertilization (dpf) (fli:GFP) Casper zebrafish embryos were put into a 24-well plate; each well contained 1 ml of egg water and different concentrations of GSK503. Six embryos were put into each well, maintained at 34 °C, and monitored daily until 8 dpf. The test was performed in triplicate and the media were refreshed every second day. When the survival was equal to or higher than 80%, the concentration was considered non-toxic to the embryos.

After choosing the appropriate concentration, the same experimental conditions were applied for the treatment of tumour cell-injected embryos. Thus, at 2 dpf, 350–450 cells of CRMM1, CRMM2 or CM2005.1 cells were injected inside the duct of Cuvier of (fli:GFP) Casper zebrafish embryos. At 1 day post-injection (dpi), drug treatment was started and continued until 6 dpi, completing a 5-day treatment. At 1 and 6 dpi, injected embryos were anaesthetized with 0.160 mg/ml tricaine (Sigma-Aldrich) to facilitate imaging under a stereo fluorescence microscope (Leica M205FA; Leica Microsystems, Amsterdam, The Netherlands.). The red pixels representing the number of cells inside the embryo were counted using ImageJ software [30].

Statistical analyses

Statistical analyses were performed with either SPSS version 23.0 software (SPSS Inc, Chicago, IL, USA) or R version 2.15.1 [31]. Pearson's chi-square, Fisher's exact, and Mann–Whitney *U*-tests were used for comparing categorical or numerical data of clinico-pathological characteristics. Two-tailed *P* values less than or equal to 0.05 were considered statistically significant. The plots of cell proliferation and cell cycle profiles were made with GraphPad Prism 6 software (GraphPad, La Jolla, CA, USA). The IC_{50} of drugs was calculated with CompuSyn software (http://www.combosyn.com), according to relative 5-day growth inhibition [32]. The effect of GSK503 *in vivo* was analysed using a generalized linear model after square-root transformation of the data.

Results

EZH2 is overexpressed in CMs and metastases

We determined EZH2 expression in CMs using IHC and analysing the intensity and percentage of positive cells. Representative samples of the different EZH2 expression patterns in CMs are shown in Figure 1 (clinico-pathological characteristics are listed in Table 1, and clinical information in the supplementary material, Table S3). In normal conjunctiva, we observed some nuclear staining of keratinocytes but not of melanocytes. EZH2 was also not expressed in PAM tissues (supplementary material, Table S4). In contrast, EZH2 was highly expressed in 13 (50%) of the CM specimens and absent or marginally expressed in the other 13 (50%) primary CMs. In addition, seven (88%) out of eight lymph node metastases of CM showed

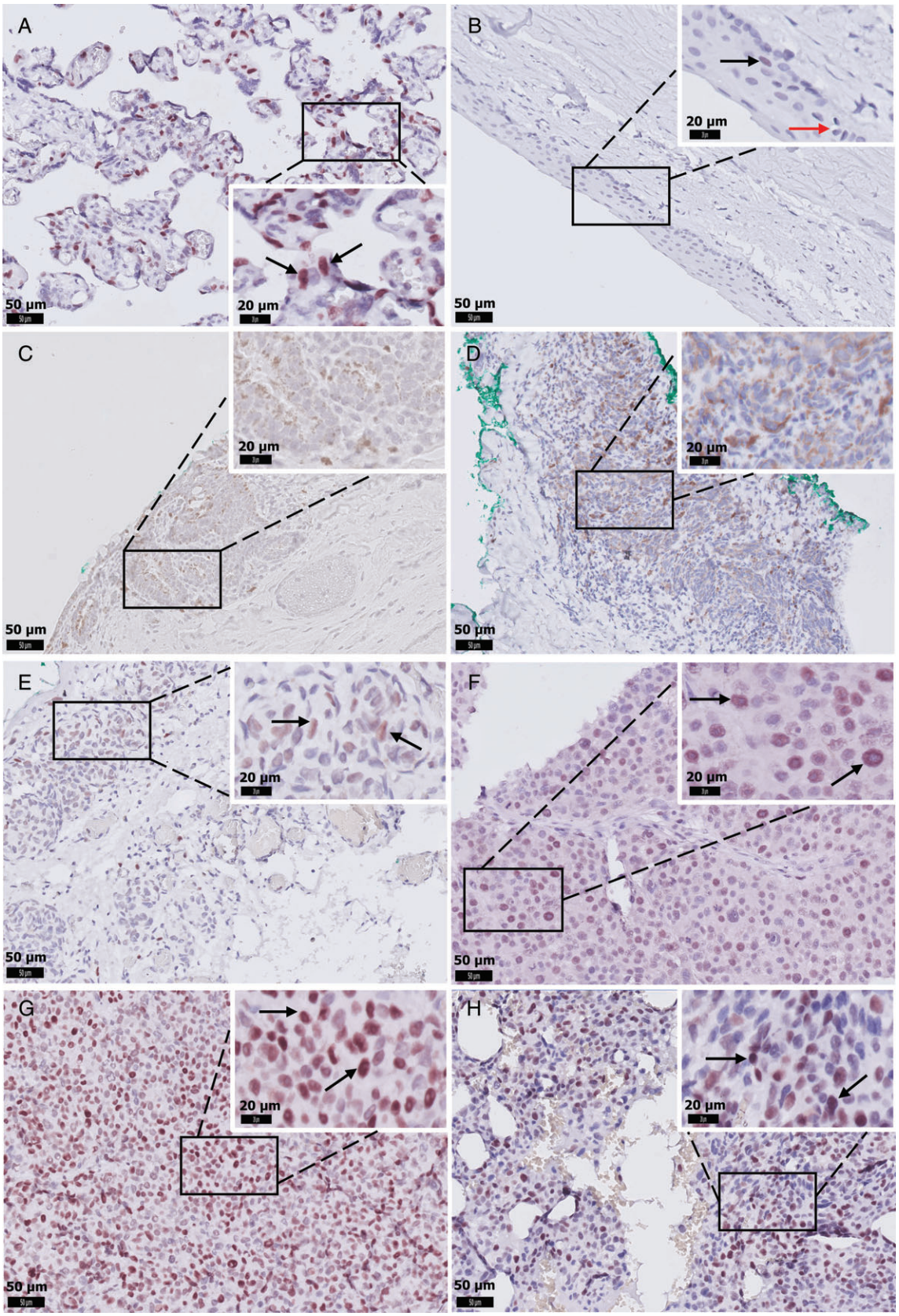

Figure 1. Representative images of EZH2 IHC staining in CM. (A) Positive control staining of placental tissue. (B) EZH2-positive keratinocytes (black arrow), and EZH2-negative melanocytes in the normal conjunctiva (red arrow). (C) EZH2 is absent in primary acquired melanosis. (D) CM with negative nuclear staining in all tumour cells. (E) CM with weak, (F) moderate, or (G) strong nuclear staining in more than 50% of tumour cells. (H) Strong nuclear staining in tumour cells in a lymph node metastasis. D and E were considered EZH2-low expression (scored ≤3); F, G, and H were scored >3 and considered EZH2-high expression. Scale bars are 50 μm (original images) and 20 μm (insets). Black arrows indicate EZH2-positive cells.

Table 1. Clinico-pathological characteristics according to low and high EZH2 expression

Characteristic	All cases Cases (%)	EZH2 low Cases (%)	EZH2 high Cases (%)	Significance *P* value
Overall	26 (100)	13 (50)	13 (50)	
Sex				
Male	11 (42)	8 (62)	3 (23)	*0.05**
Female	15 (58)	5 (38)	10 (77)	
Age at diagnosis				
Median (range), years	60.3 (21.2–86.3)	56.5 (21.2–73.0)	67.1 (48.7–86.3)	*0.03***
Tumour size, thickness	*N* = 23	*N* = 11	*N* = 12	
Median (range), mm	1.0 (0.1–16.0)	0.6 (0.2–2.5)	3.3 (0.1–16.0)	*0.03***
Tumour size, LBD	*N* = 23	*N* = 13	*N* = 10	
Median (range), mm	10.0 (2.0–30.0)	9.0 (2.0–30.0)	11.0 (5.0–20.0)	0.45**
Location				
Epibulbar	19 (73)	11 (85)	8 (62)	0.38†
Non-epibulbar	7 (27)	2 (15)	5 (38)	
cTNM				
T1	19 (73)	11 (85)	8 (62)	0.38†
T2	7 (27)	2 (15)	5 (38)	
Local recurrence				
No	16 (62)	7 (54)	9 (69)	0.42*
Yes	10 (38)	6 (46)	4 (31)	
Distant metastasis				
No	23 (88)	12 (92)	11 (85)	1.00†
Yes	3 (12)	1 (8)	2 (15)	

LBD = largest basal diameter; cTNM = clinical TNM stage, based on the first occurring conjunctival melanoma.
P value calculation: *Pearson's chi-square; **Mann–Whitney *U*-test; †Fisher's exact test. Italic *P* values ≤0.05. The scoring method for EZH2 is described in the Materials and methods section.

strong EZH2 expression (supplementary material, Table S5). In primary tumours, EZH2 expression correlated positively with tumour thickness ($p = 0.03$). A high level of EZH2 expression was correlated with worse overall survival and tended to be associated with worse melanoma-related survival (Figure 2). However, EZH2 expression was not correlated with tumour location, tumour stage, local recurrence or distant metastasis (Table 1).

Pharmacological inhibition of EZH2 in CM cells

We determined EZH2 protein expression in three CM cell lines, a cutaneous melanocyte cell culture (07-11), and two cutaneous melanoma cell lines, one of which (A375) has previously been used extensively in determining the function of EZH2 [33]. Compared with the normal cutaneous melanocytes, all melanoma cell lines overexpressed EZH2 (Figure 3A). To investigate a putative growth stimulatory function of EZH2 in CM, we treated the cells with the small molecule EZH2 inhibitors GSK503 and UNC1999, since these had been shown to successfully inhibit the function of EZH2 in lymphoma and cutaneous melanoma *in vitro* and *in vivo* [20,34]. Figure 3B, F shows that the level of H3K27me3 in CM cells decreased following increasing concentrations of GSK503 and UNC1999. EZH2 expression in CRMM2 and CM2005.1 was slightly decreased by GSK503, and UNC1999 clearly reduced EZH2 expression in CRMM2 at a high concentration (6 μM). IC_{50} values are shown in Table 2.

It has been reported that *EZH2* depletion increases p21 expression in cancer cell lines and thereby induces cellular senescence [35,36]. Therefore, we examined p21 expression after drug treatment. However, we found that the p21 protein levels were only marginally elevated in CRMM1 and CM2005.1 cell lines exposed to either drug. Basal levels of p21 are very high in CRMM2 and the increase is hard to evaluate. Treatment for 5 days with GSK503 reduced the relative survival of CM cells, although the inhibitory effects on CM2005.1 cells required higher concentrations than the other cell lines (Figure 3C). Similarly, the proliferation of all CM cell lines was suppressed following UNC1999 treatment (Figure 3G). The colony formation assay confirmed the findings of the cell growth assay (supplementary material, Figure S1).

Genes such as *p14ARF*, *p16INK4a*, *p21/CDKN1A*, and *p27KIP1* have been described as targets of EZH2 inhibition in several cancer types [35,37]. We therefore investigated whether GSK503 or UNC1999 affected the transcription of these genes in CM cells. However, the mRNA levels of *p14ARF*, *p16INK4a*, *p21/CDKN1A*, and *p27KIP1* were not significantly affected by these drugs (supplementary material, Figure S2). Nevertheless, our results show that CM2005.1 does not express *p14ARF* or *p16INK4a*, while CRMM2 lacks *p16INK4a* expression.

To determine the effects of EZH2 inhibition on cell cycle and apoptosis, we performed flow cytometry analysis after propidium iodide staining (Figure 3D, H) and western blot analysis to investigate PARP cleavage (Figure 3E, I). Flow cytometry analysis of GSK503-treated CRMM1 and CRMM2 cells demonstrated a G1 arrest concomitant with S-phase depletion and slightly increased numbers of sub-G1 cells. In CM2005.1, on the other hand, we noticed an increase in the proportion of cells in the G2/M phase (Figure 3D),

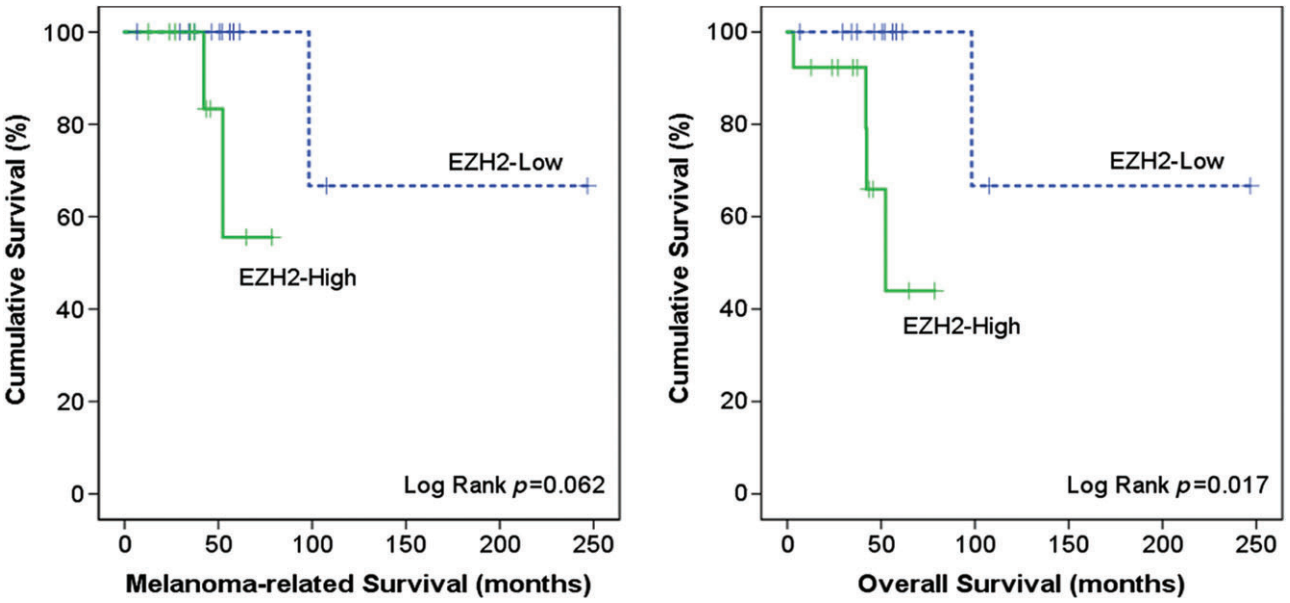

Figure 2. Kaplan–Meier analysis of melanoma-related and overall survival based on EZH2 expression.

also with an increase in the sub-G1 fraction. Some cleaved PARP could be detected in lysates from treated CRMM1 and CM2005.1 cells (Figure 3E). Following UNC1999 treatment, CRMM1 and CRMM2 cells showed an S-phase reduction concomitant with an increase of G1-phase cells. Furthermore, more sub-G1 cells were observed, indicating cell death (Figure 3H). In CM2005.1 cells, UNC1999 exposure did not have a strong effect on the cell cycle profile, but possibly the cells progress more slowly through the S-phase as that fraction is somewhat increased. A clearly increased sub-G1 fraction was identified, again indicating cell death. After UNC1999 treatment, no upregulation of cleaved PARP was observed in any cell line (Figure 3I), which may indicate that the observed cell death is not via induction of apoptosis. To determine whether the observed cell death following UNC1999 treatment was still correlated with changes in the expression of key apoptotic proteins, we performed western blot analyses. Although we did find some effects of UNC1999 treatment on the levels of Mcl-1, Bcl-XL, Bcl-2, PUMA, Bim, survivin, and E2F1 (supplementary material, Figure S3), the effects were not consistent in the three cell lines. Since EZH2 has also been linked to the regulation of autophagy [38], the lysates of the three CM cell lines treated for 5 days with GSK503 or UNC1999 were investigated for expression of LC3B-II, a hallmark of autophagy [39]. Protein expression of LC3B-II was increased in CM cells upon GSK503 and UNC1999 treatment, although at different levels (Figure 3J), suggesting the induction of autophagy.

Effect of *EZH2* knockdown in CM cells

Next, to genetically validate the findings of catalytic EZH2 inhibitors, we specifically depleted *EZH2* in melanoma cell lines using lentiviral-expressed short hairpin RNAs (shRNAs). Expression of EZH2 was significantly decreased in sh-*EZH2*-expressing cells compared with control transduced cells (shc002, shc007), correlating with a global decrease of H3K27me3 (Figure 4A). This confirmed that H3K27me3 was largely dependent on the presence of EZH2. Depletion of *EZH2* increased p21 protein levels in CRMM1, CRMM2 (shEZH2 20), and CM2005.1, suggesting that the cellular senescence marker p21 participates in growth repression of CM cell lines. Activation of *p21/CDKN1A* transcription was detected in most *EZH2*-depleted cells, although some variation between cell lines and *EZH2* shRNAs was observed (Figure 4B). We also investigated the mRNA expression of *p16INK4a*, *p14ARF*, and *p27KIP1*, but their expression was not affected by *EZH2* depletion (data not shown).

Importantly, the in-cell western assay indicated a lower proliferation of *EZH2* shRNA-treated cells compared with control shRNA-treated cells (Figure 4C). Knockdown of *EZH2* also strongly decreased the ability of CM cells to form colonies (supplementary material, Figure S4). Flow cytometry analyses showed that in CRMM1 and CRMM2, *EZH2* knockdown resulted in S-phase depletion with G1 arrest (Figure 4D). Interestingly, in CM2005.1, *EZH2* depletion mainly caused an accumulation of cells in G2/M. In addition, an increased sub-G1 fraction was observed in all *EZH2*-depleted cells, suggesting that EZH2 protects CM cells from cell death.

Western blotting showed that *EZH2* knockdown increased the amount of cleaved PARP in CM cell lines. It should be noted that the full-length PARP expression in CRMM2 cells upon *EZH2* depletion was strongly reduced, which may suggest that PARP is cleaved and that the cleaved product is unstable. In general, *EZH2* depletion induced some degree of apoptosis in CM cells, indicating its importance in cell survival. The

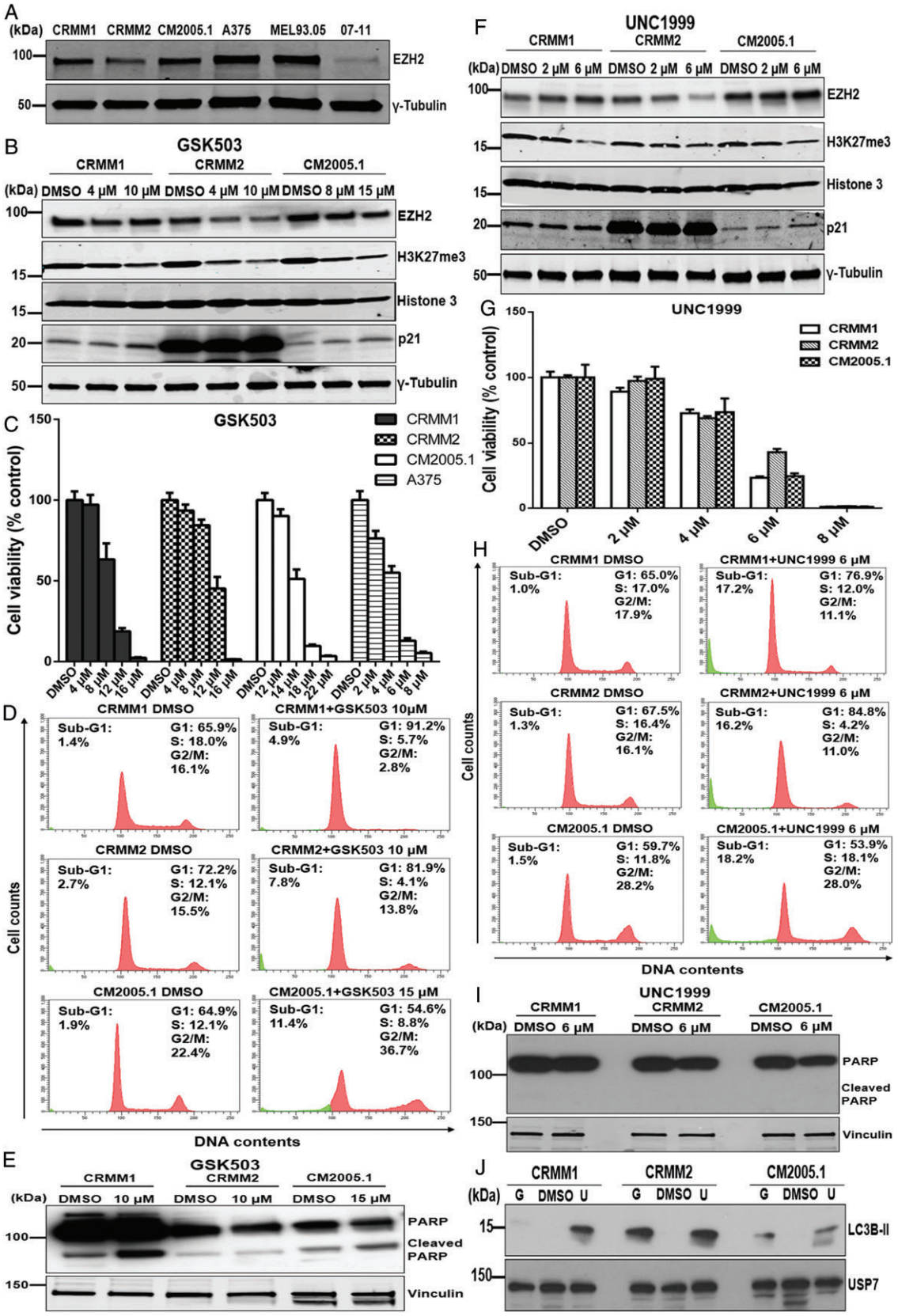

Figure 3. Effect of the EZH2 inhibitors GSK503 and UNC1999 on CM cell lines. (A) Western blot analysis of EZH2 protein in three CM cell lines, CRMM1, CRMM2, and CM2005.1, and two cutaneous melanoma cell lines, A375 and MEL93.05; 07-11 is a human melanocyte culture. Western blot analysis of CM cells upon 120 h incubation of GSK503 (B) or UNC1999 (F) treatment. Representative bar graphs show the proliferation of melanoma cell lines exposed for 120 h to GSK503 (C) or UNC1999 (G), respectively. The intensity (*Y* axis) was normalized to DMSO-treated control cells. Data are presented as means ±SEM from one representative experiment. Histograms represent DNA content (D, H) and western blot analysis of (cleaved) PARP (E, J) following 120 h incubation of GSK503 or UNC1999. (J) LC3B-II levels are increased following 120 h treatment of GSK503 (G, CRMM1 and CRMM2 at 10 μM, and CM2005.1 at 15 μM) or UNC1999 (U, 6 μM).

Table 2. Cell growth IC_{50} of EZH2 inhibitors in CM cell lines

Cell line	GSK503 (μM)	UNC1999 (μM)
CRMM1	8.5 ± 0.4	4.2 ± 0.3
CRMM2	9.3 ± 0.7	4.1 ± 0.4
CM2005.1	15.9 ± 1.4	4.4 ± 0.3

Cell viability IC_{50} values of GSK503 ($n = 3$) and UNC1999 ($n = 2$) in CM cell lines (in-cell western assay) were determined based on relative 5-day survival.

results obtained upon *EZH2* depletion are strongly reminiscent of the data obtained with the GSK503 inhibitor (Figure 3D, E), suggesting that this inhibitor indeed mainly acts through inhibition of EZH2 activity, while UNC1999 might have additional activities [40].

Therapeutic effect of GSK503 in a zebrafish model

To confirm the findings obtained in cell culture, we established a zebrafish model to test the drug GSK503 *in vivo*. A well-tolerated concentration of GSK503 was determined as previously described [41]. Concentrations of GSK503 were non-toxic to the embryos until at least 8 dpf (supplementary material, Figure S5), as over 80% of the embryos survived during the observation period, even at the highest concentration (24 μM). Subsequently, three CM cell lines expressing tomato red were injected into the duct of Cuvier of (fli:GFP) Casper zebrafish embryos at 2 dpf, and treatment with 24 μM GSK503 or DMSO diluted in egg water was initiated at 1 dpi and continued until 6 dpi (5-day treatment). Next, cell growth and dissemination were scored by counting the number of red pixels in the embryos. Figure 5 shows that tumour cells migrated to other areas through the blood circulation and proliferated. Importantly, the tumour burden of all three CM cell lines *in vivo* was significantly reduced after the 5-day treatment with GSK503. We tested the difference between the control and the treated groups of the zebrafish embryos injected with the three CM cell lines with a generalized linear model: the *P* values were 0.015 (CRMM1), 0.002 (CRMM2), and 0.028 (CM2005.1).

Discussion

To the best of our knowledge, this is the first study that demonstrates the importance of EZH2 in CM. Here, we report that EZH2 is overexpressed in CM. EZH2 was expressed on keratinocytes of normal conjunctiva, but not on cells of melanocytic lineage. This is consistent with studies of cutaneous melanoma, which similarly showed that EZH2 is present in epidermal keratinocytes, but absent or expressed at low level in naevi and epidermal melanocytes [20,42]. Interestingly, although many CMs develop in association with PAM [4], EZH2 was not expressed in PAM. Importantly, we demonstrate that EZH2 expression is detected in a significant proportion of CMs and is positively associated with one of the prognostic factors, tumour thickness [4]. Furthermore, EZH2 was highly expressed in most lymph node metastases. Taken together, our findings indicate that EZH2 protein levels are often increased in CM and metastases, and EZH2 may therefore be involved in the pathogenesis and progression of CM tumours.

Many small molecule inhibitors targeting EZH2 have been developed to block its catalytic activity, i.e. EZH2-mediated methylation of H3K27. A phase 1/2 clinical trial of tazemetostat (EPZ-6438) is currently ongoing against advanced solid tumours and B-cell lymphoma (NCT 01897571). In the present study, we applied two EZH2 inhibitors, GSK503 and UNC1999, to CM cell lines. In addition, we utilized genetic knockdown to confirm the findings of the pharmacological depletion of *EZH2*. Interestingly, expression of the tumour suppressor gene *p21/CDKN1A* was more convincingly upregulated in *EZH2*-knockdown CM cells than in inhibitor-treated cells, suggesting that EZH2 has function(s) in transcription regulation independent of its catalytic activity. It is known that the mechanisms of EZH2 oncogenic activity are cancer type-dependent, including the canonical role of EZH2 in gene silencing in cutaneous melanoma and colon cancer, and the non-canonical function of EZH2 that affects other pathways in a histone methylation-independent manner. For example, EZH2 can trigger NF-κB signalling in basal-like breast cancer and transcriptionally co-activate the androgen receptor in castration-resistant prostate cancer [43,44]. Further studies are warranted to elucidate the function(s) of EZH2 in CM. Regarding the cell cycle profile and apoptosis, drug treatment and RNA interference (RNAi) similarly resulted in G1 arrest and S-phase depletion in CRMM1 and CRMM2. GSK503 and UNC1999 appeared to induce cell death via partly different mechanisms. Similar to the genetic depletion of *EZH2*, the GSK503 inhibitor activated apoptosis and possibly some autophagy. However, increased caspase activity as monitored by PARP cleavage could not be detected upon UNC1999 treatment and no consistent effect on the level of several key proteins in apoptotic pathways could be detected, but our results suggest induction of autophagy. Different patterns of cell death displayed by these treatments suggest that pharmaceutical inhibition cannot totally mimic the *EZH2* knockdown in this scenario. Discrepancies between genetic knockdown and enzymatic inhibitors of EZH2 on biological outcome have been described before: it was reported that catalytic inhibition of EZH2 using GSK343 and GSK126 induced no or modest expression of interferon gamma receptor 1 despite effective inhibition of H3K27me3 in a prostate cancer cell line, in contrast to depletion of EZH2 expression [45]. Similarly, it was found that SWI/SNF-mutant cancer lines are more sensitive to *EZH2* knockdown than to catalytic inhibitors [46]. Regarding the autophagy context, the accumulation of LC3B-II may indicate that EZH2 inhibitors induce autophagy in CM cells, although induction of autophagy may either increase or repress cell growth, depending on the stage of tumourigenesis and mutational and oncogenic background [47]. Hsieh *et al* have shown that the promotion of cell death by

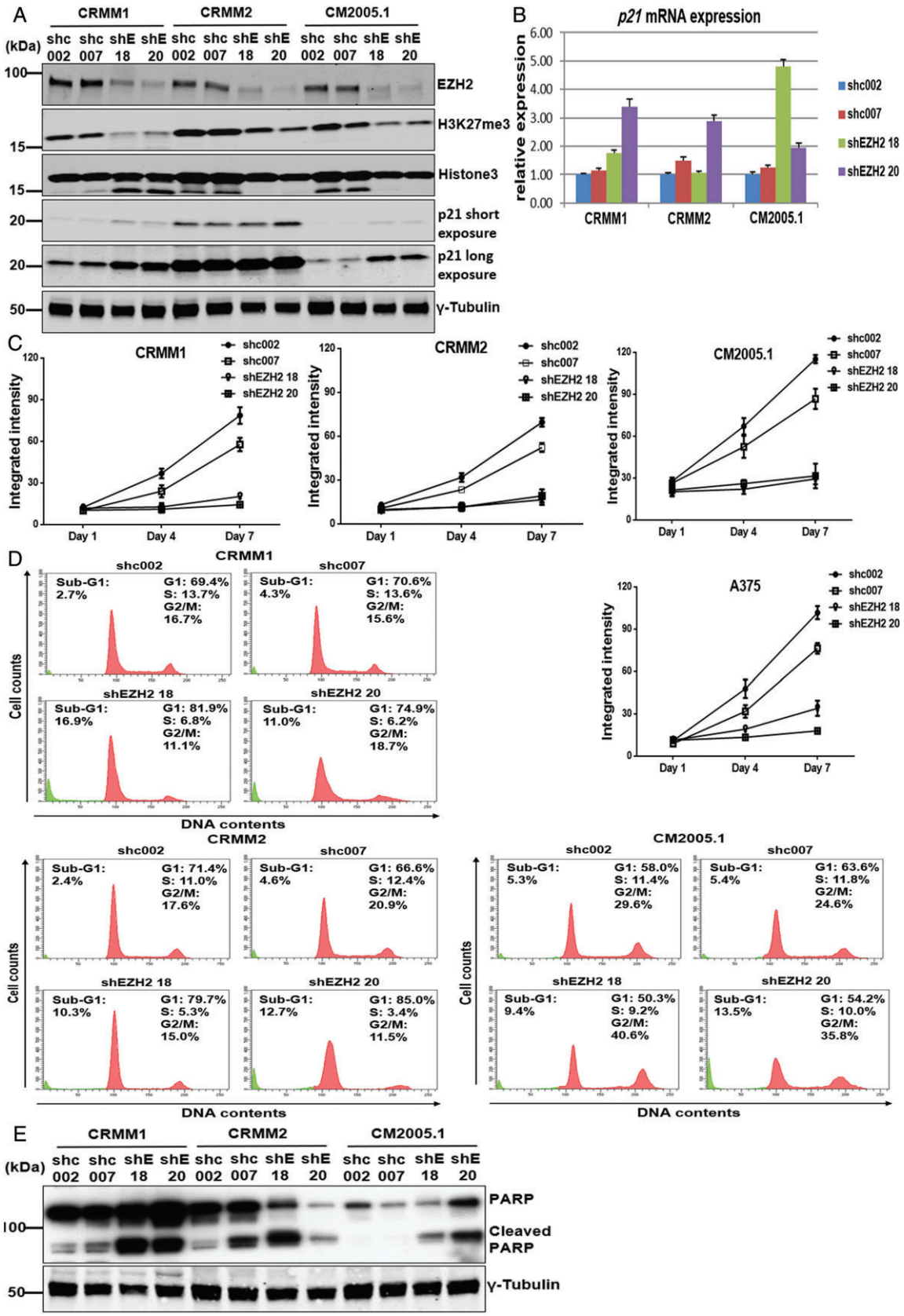

Figure 4. *EZH2* knockdown reduces H3K27me3, elevates p21 expression, suppresses cell growth, and induces cell cycle arrest and apoptosis in CM. (A) The expression of EZH2, H3K27me3, and cell cycle regulatory protein p21 was determined upon *EZH2* depletion using shEZH2 18, shEZH2 20, and compared with control shRNAs (shc002 and shc007) 72 h after puromycin selection. (B) The mRNA expression of *p21* was increased upon *EZH2* knockdown. (C) Representative growth curves of CM cell lines and the A375 cell line after *EZH2* knockdown by specific *EZH2* shRNAs compared with control shRNAs. Error bars indicate the standard deviation. (D) Histograms show the percentages of CRMM1, CRMM2, and CM2005.1 cells in specific cell cycle phases, and western blot analyses (E) (cleaved) PARP in CM cells upon *EZH2* knockdown.

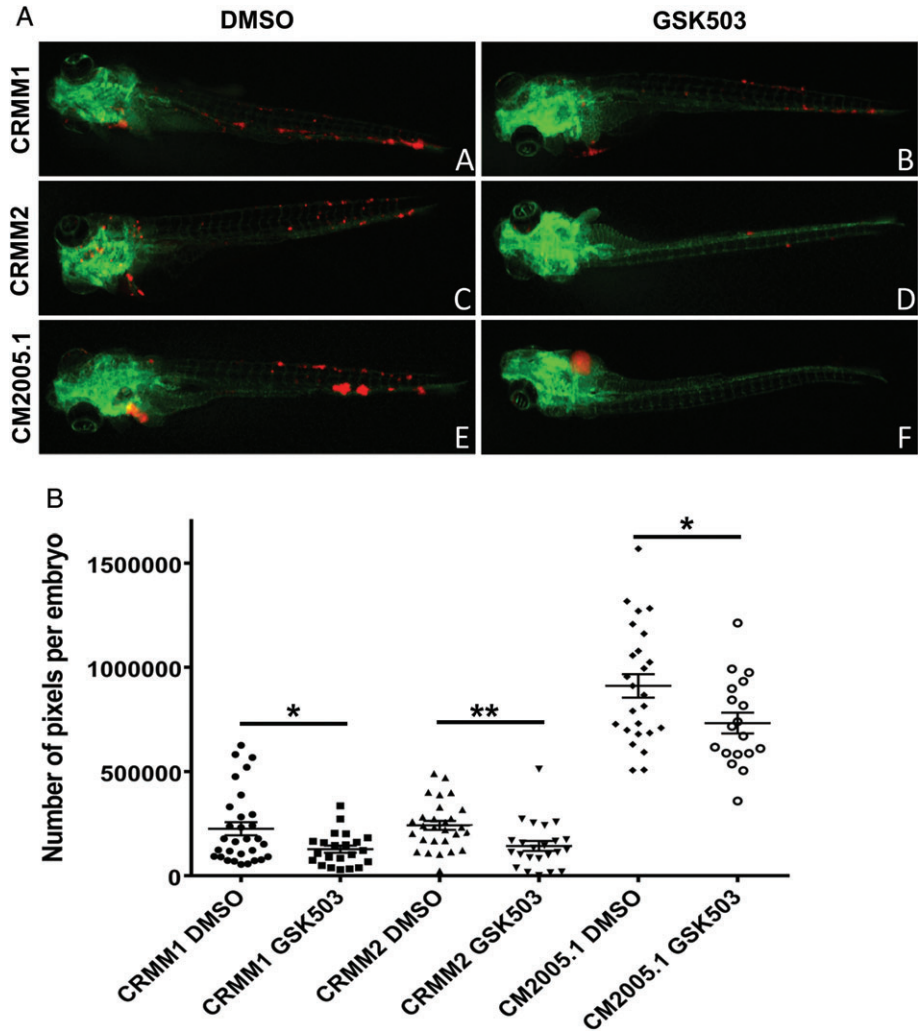

Figure 5. GSK503 suppresses the growth of CM cell lines in a zebrafish model. CM cells were labelled with tomato red (red) and injected into the duct of Cuvier at 2 dpf in (fli:GFP) Casper zebrafish embryos, which have a green vasculature. The images were taken at 6 dpi. (A, black) Representative stereo fluorescent images (original magnification: 20 ×) show inhibition of tumour growth after exposure to 24 μM GSK503. (B, black) Number of red pixels represent tumour cells with DMSO or GSK503 treatment in CM xenografts. Each point indicates one embryo and its corresponding pixel count. Statistical significance was calculated by the generalized linear model and *P* values are indicated as follows: $^{*}p < 0.05$, $^{**}p < 0.01$. $N_{CRMM1/DMSO} = 30$, $N_{CRMM1/GSK503} = 22$, $N_{CRMM2/DMSO} = 28$, $N_{CRMM2/GSK503} = 23$, $N_{CM2005.1/DMSO} = 25$, $N_{CM2005.1/GSK503} = 18$.

autophagy upon treatment with GSK343 or UNC1999 occurred independently of EZH2 inhibition [40]. This may explain why *EZH2* knockdown and UNC1999 treatment have partly distinct effects.

Our newly developed zebrafish xenograft model allowed the tumour cells to disseminate, and therefore served as an efficient model of metastatic spread. After inoculation into the blood circulation, tumour cells spread to the head and tail of the zebrafish and proliferated, allowing further drug tests. GSK503 profoundly reduced the growth of CM cells at a well-tolerated concentration. To the best of our knowledge, this is the first report using an animal model to test an epigenetic inhibitor in CM. Although one might question the relevance of a zebrafish model for human patients, Howe *et al* recently showed that approximately 71% of human genes have a corresponding zebrafish ortholog using the Zv9 assembly. Conversely, 69% of zebrafish genes have at least one human ortholog [48]. Integrins and other adhesion molecules form a critical adhesion point for cancer cells and play a crucial role in the metastatic initiation of a plethora of cancers [49]. While integrins enable extracellular matrix interactions required for metastatic initiation, cadherin molecules function as homotypic cell–cell adhesion molecules. Cadherins predominantly play a role in metastatic outgrowth and progression [50]. In many solid tumours, loss of E-cadherin is seen as a key turning point in disease progression enabling cells to dissociate from the primary tumour and metastasize [51]. Zebrafish integrins are in general highly homologous to their human counterparts, whereas the functional majority of cadherins are conserved in all metazoans [52].

Overall, our results demonstrate that EZH2 is overexpressed in CM and lymph node metastases compared with normal conjunctival melanocytes and PAM, and

that high EZH2 protein levels are associated with tumour thickness and overall survival. Both pharmaceutical compounds ands RNAi targeting EZH2 repressed the growth of CM cells in culture and *in vivo*. Taken together, these data reveal that EZH2-targeted therapy may be a potential therapeutic strategy for patients with CM.

Acknowledgements

We thank Marja van Eggermond (IHB, LUMC, The Netherlands) for providing information regarding EZH2 and H3K27me3 antibodies, and Catalina Gomez Puerto (MCB, LUMC, The Netherlands) for sharing anti-p62 and anti-LC3B-II antibodies.

Author contributions statement

MJJ initiated the idea, obtained funding, and critically revised the manuscript. AGJ participated in setting up and performing the experiments, and revising the manuscript. JC performed the *in vitro* experiments, analysed the results, and wrote the manuscript. KCP and AG established the animal model and performed *in vivo* studies. RCH and AFT were involved in *in vitro* experiments. ESJ scored the slides. NJB collected clinical information and performed statistical analyses. RMV, MM, and SD gave technical and material support.

References

1. Tuomaala S, Eskelin S, Tarkkanen A, *et al.* Population-based assessment of clinical characteristics predicting outcome of conjunctival melanoma in whites. *Invest Ophthalmol Vis Sci* 2002; **43:** 3399–3408.
2. Yu GP, Hu DN, McCormick S, *et al.* Conjunctival melanoma: is it increasing in the United States? *Am J Ophthalmol* 2003; **135:** 800–806.
3. Triay E, Bergman L, Nilsson B, *et al.* Time trends in the incidence of conjunctival melanoma in Sweden. *Br J Ophthalmol* 2009; **93:** 1524–1528.
4. Shields CL, Shields JA, Gunduz K, *et al.* Conjunctival melanoma: risk factors for recurrence, exenteration, metastasis, and death in 150 consecutive patients. *Arch Ophthalmol* 2000; **118:** 1497–1507.
5. Missotten GS, Keijser S, De Keizer RJ, *et al.* Conjunctival melanoma in the Netherlands: a nationwide study. *Invest Ophthalmol Vis Sci* 2005; **46:** 75–82.
6. Werschnik C, Lommatzsch PK. Long-term follow-up of patients with conjunctival melanoma. *Am J Clin Oncol* 2002; **25:** 248–255.
7. Griewank KG, Westekemper H, Murali R, *et al.* Conjunctival melanomas harbor *BRAF* and *NRAS* mutations and copy number changes similar to cutaneous and mucosal melanomas. *Clin Cancer Res* 2013; **19:** 3143–3152.
8. Cao J, Heijkants RC, Jochemsen AG, *et al.* Targeting of the MAPK and AKT pathways in conjunctival melanoma shows potential synergy. *Oncotarget* 2016; **8:** 58021–58036.
9. Pahlitzsch M, Bertelmann E, Mai C. Conjunctival melanoma and BRAF inhibitor therapy. *J Clin Exp Ophthalmol* 2014; **5:** 322.
10. Maleka A, Åström G, Byström P, *et al.* A case report of a patient with metastatic ocular melanoma who experienced a response to treatment with the BRAF inhibitor vemurafenib. *BMC Cancer* 2016; **16:** 634.
11. Varambally S, Dhanasekaran SM, Zhou M, *et al.* The polycomb group protein EZH2 is involved in progression of prostate cancer. *Nature* 2002; **419:** 624–629.
12. Bachmann IM, Halvorsen OJ, Collett K, *et al.* EZH2 expression is associated with high proliferation rate and aggressive tumour subgroups in cutaneous melanoma and cancers of the endometrium, prostate, and breast. *J Clin Oncol* 2006; **24:** 268–273.
13. Ciferri C, Lander GC, Maiolica A, *et al.* Molecular architecture of human polycomb repressive compex 2. *eLife* 2012; **1:** e00005.
14. Riquelme E, Behrens C, Lin HY, *et al.* Modulation of EZH2 expression by MEK-ERK or PI3K-AKT signaling in lung cancer is dictated by different KRAS oncogene mutations. *Cancer Res* 2016; **76:** 675–685.
15. Konze KD, Ma A, Li F, *et al.* An orally bioavailable chemical probe of the lysine methyltransferases EZH2 and EZH1. *ACS Chem Biol* 2013; **8:** 1324–1334.
16. Kim KH, Roberts CW. Targeting EZH2 in cancer. *Nat Med* 2016; **22:** 128–133.
17. Knutson SK, Wigle TJ, Warholic NM, *et al.* A selective inhibitor of EZH2 blocks H3K27 methylation and kills mutant lymphoma cells. *Nat Chem Biol* 2012; **8:** 890–896.
18. Bradley WD, Arora S, Busby J, *et al.* EZH2 inhibitor efficacy in non-Hodgkin's lymphoma does not require suppression of H3K27 monomethylation. *Chem Biol* 2014; **21:** 1463–1475.
19. Tiffen J, Gallagher SJ, Hersey P. EZH2: an emerging role in melanoma biology and strategies for targeted therapy. *Pigment Cell Melanoma Res* 2015; **28:** 21–30.
20. Zingg D, Debbache J, Schaefer SM, *et al.* The epigenetic modifier EZH2 controls melanoma growth and metastasis through silencing of distinct tumour suppressors. *Nat Commun* 2015; **6:** 6051.
21. Edge SB, Byrd DR, Compton CC, *et al* (eds). Malignant melanoma of the conjunctiva. In *AJCC Cancer Staging Manual* (7th edn). Springer: New York, 2010; 539–546.
22. Cao J, Brouwer NJ, Richards KE, *et al.* PD-L1/PD-1 expression and tumor-infiltrating lymphocytes in conjunctival melanoma. *Oncotarget* 2017; **8:** 54722–54734.
23. Reijm EA, Timmermans AM, Look MP, *et al.* High protein expression of EZH2 is related to unfavorable outcome to tamoxifen in metastatic breast cancer. *Ann Oncol* 2014; **25:** 2185–2190.
24. Nareyeck G, Wuestemeyer H, von der Haar D, *et al.* Establishment of two cell lines derived from conjunctival melanomas. *Exp Eye Res* 2005; **81:** 361–362.
25. Keijser S, Maat W, Missotten GS, *et al.* A new cell line from a recurrent conjunctival melanoma. *Br J Ophthalmol* 2007; **91:** 1566–1567.
26. Carlotti F, Bazuine M, Kekarainen T, *et al.* Lentiviral vectors efficiently transduce quiescent mature 3T3-L1 adipocytes. *Mol Ther* 2004; **9:** 209–217.
27. Lawson ND, Weinstein BM. *In vivo* imaging of embryonic vascular development using transgenic zebrafish. *Dev Biol* 2002; **248:** 307–318.
28. Pontes KC, Groenewoud A, Cao J, *et al.* Evaluation of (*fli:GFP*) *Casper* zebrafish embryos as a model for human conjunctival melanoma. *Invest Ophthalmol Vis Sci* 2017; **58:** 6065–6071.
29. White RM, Sessa A, Burke C, *et al.* Transparent adult zebrafish as a tool for *in vivo* transplantation analysis. *Cell Stem Cell* 2008; **2:** 183–189.
30. Schneider CA, Rasband WS, Eliceiri KW. NIH Image to ImageJ: 25 years of image analysis. *Nat Methods* 2012; **9:** 671–675.
31. R Core Team. *R: A language and environment for statistical computing*. R Foundation for Statistical Computing, Vienna, Austria. [Accessed 2013]. Available from: http://www.R-project.org/
32. Chou TC, Martine N. *CompuSyn for Drug Combinations. PC Software and User's Guide*. ComboSyn Inc, Paramus, NJ, 2005.

33. Barsotti AM, Ryskin M, Zhong W, *et al.* Epigenetic reprogramming by tumour-derived EZH2 gain-of-function mutations promotes aggressive 3D cell morphologies and enhances melanoma tumor growth. *Oncotarget* 2015; **6:** 2928–2938.
34. Xu B, On DM, Ma A, *et al.* Selective inhibition of EZH2 and EZH1 enzymatic activity by a small molecule suppresses MLL-rearranged leukemia. *Blood* 2015; **125:** 346–357.
35. Fan T, Jiang S, Chung N, *et al.* EZH2-dependent suppression of a cellular senescence phenotype in melanoma cells by inhibition of p21/CDKN1A expression. *Mol Cancer Res* 2011; **9:** 418–429.
36. Xia H, Zhang W, Li Y, *et al.* EZH2 silencing with RNA interference induces G2/M arrest in human lung cancer cells *in vitro*. *Biomed Res Int* 2014; **2014:** 348728.
37. Sha MQ, Zhao XL, Li L, *et al.* EZH2 mediates lidamycin-induced cellular senescence through regulating p21 expression in human colon cancer cells. *Cell Death Dis* 2016; **7:** e2486.
38. Wei FZ, Cao Z, Wang X, *et al.* Epigenetic regulation of autophagy by the methyltransferase EZH2 through an MTOR-dependent pathway. *Autophagy* 2015; **11:** 2309–2322.
39. Mizushima N, Yoshimori T. How to interpret LC3 immunoblotting. *Autophagy* 2007; **3:** 542–545.
40. Hsieh YY, Lo HL, Yang PM. EZH2 inhibitors transcriptionally upregulate cytotoxic autophagy and cytoprotective unfolded protein response in human colorectal cancer cells. *Am J Cancer Res* 2016; **6:** 1661–1680.
41. van der Ent W, Burrello C, Teunisse AF, *et al.* Modeling of human uveal melanoma in zebrafish xenograft embryos. *Invest Ophthalmol Vis Sci* 2014; **55:** 6612–6622.
42. McHugh JB, Fullen DR, Ma L, *et al.* Expression of polycomb group protein EZH2 in nevi and melanoma. *J Cutan Pathol* 2007; **34:** 597–600.
43. Lee ST, Li Z, Wu Z, *et al.* Context-specific regulation of NF-κB target gene expression by EZH2 in breast cancers. *Mol Cell* 2011; **43:** 798–810.
44. Xu K, Wu ZJ, Groner AC, *et al.* EZH2 oncogenic activity in castration-resistant prostate cancer cells is Polycomb-independent. *Science* 2012; **338:** 1465–1469.
45. Wee ZN, Li Z, Lee PL, *et al.* EZH2-mediated inactivation of IFN-γ–JAK–STAT1 signaling is an effective therapeutic target in MYC-driven prostate cancer. *Cell Rep* 2014; **8:** 204–216.
46. Kim KH, Kim W, Howard TP, *et al.* SWI/SNF-mutant cancers depend on catalytic and non-catalytic activity of EZH2. *Nat Med* 2015; **21:** 1491–1496.
47. Towers CG, Thorburn A. Therapeutic targeting of autophagy. *EBioMedicine* 2016; **14:** 15–23.
48. Howe K, Clark MD, Torroja CF, *et al.* The zebrafish reference genome sequence and its relationship to the human genome. *Nature* 2013; **496:** 498–503.
49. Seguin L, Desgrosellier JS, Weis SM, *et al.* Integrins and cancer: regulators of cancer stemness, metastasis, and drug resistance. *Trends Cell Biol* 2015; **25:** 234–240.
50. Jeanes A, Gottardi CJ, Yap AS. Cadherins and cancer: how does cadherin dysfunction promote tumor progression? *Oncogene* 2008; **27:** 6920–6929.
51. Onder TT, Gupta PB, Mani SA, *et al.* Loss of E-cadherin promotes metastasis via multiple downstream transcriptional pathways. *Cancer Res* 2008; **68:** 3645–3654.
52. Schmalhofer O, Brabletz S, Brabletz T. E-cadherin, beta-catenin, and ZEB1 in malignant progression of cancer. *Cancer Metastasis Rev* 2009; **28:** 151–166.

SUPPLEMENTARY MATERIAL ONLINE

Supplementary materials and methods

Figure S1. GSK503 and UNC1999 inhibit colony formation in melanoma cell lines

Figure S2. GSK503 and UNC1999 do not alter the mRNA levels of *p14ARF*, *p16*, *p21* or *p27* in CM cell lines

Figure S3. Western blot analysis of several key apoptotic proteins after UNC1999 treatment

Figure S4. EZH2 depletion inhibits colony formation of three CM cell lines and A375

Figure S5. Toxicity test of GSK503 in zebrafish

Table S1. Primary antibodies used for western blotting

Table S2. List of the primers used

Table S3. Clinical information of the patients

Table S4. EZH2 score of PAM

Table S5. EZH2 score of lymph node metastases